ACS APPLIED MATERIALS & INTERFACES

Letter

www.acsami.org

Vertical-Interface-Manipulated Conduction Behavior in Nanocomposite Oxide Thin Films

Weiwei Li,[†] Run Zhao,[†] Rujun Tang,[†] Aiping Chen,[‡] Wenrui Zhang,[‡] Xin Lu,[†] Haiyan Wang,[‡] and Hao Yang*[,†]

[†]School of Physical Science and Technology & Collaborative Innovation Center of Suzhou Nano Science and Technology, Soochow University, Suzhou 215006, China

[‡]Department of Electrical and Computer Engineering, Texas A&M University, College Station, Texas 77843-3128, United States

ABSTRACT: Vertically aligned nanocomposites with vertical interfaces are a novel concept that show powerful advantages over conventional nanocomposites with lateral interfaces. However, significant obstacles to a systematic understanding of vertical interfaces still remain. Here, heteroepitaxial $(BaTiO_3)_{0.5}$:$(Sm_2O_3)_{0.5}$ nanocomposite thin films have been fabricated and the conduction behaviors have been investigated. A spontaneous phase ordering with clear vertical interfaces has been found in the composite films. Because of the structural discontinuity as well as a large strain generated at the interfaces, the vertical interfaces are revealed to become the sinks to attract oxygen vacancies. The accumulated oxygen vacancies contributed to a largely reduced leakage current and a different leakage mechanism in the composite films compared to that of the pure $BaTiO_3$ film. The present work represents a methodology to manipulate functionalities by designing configuration of the interfaces in oxide thin films.

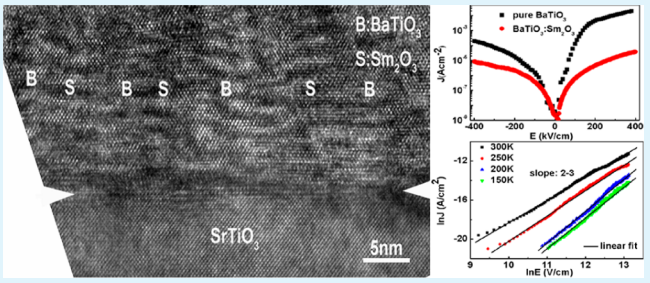

KEYWORDS: *vertically aligned nanocomposites, heteroepitaxial thin films, vertical interfaces, oxygen vacancies, conduction behavior, leakage current*

Oxide interfaces have been proven to be able to offer tremendous opportunities for fundamental as well as applied research.[1] They are of great interest because of rich interaction between charge, orbital, spin, and lattice at the interfaces. These behaviors contributed to pronounced phenomena such as quantum Hall effect and superconductivity, etc.[2] The conventional oxide interfaces are usually introduced by layer-by-layer growth techniques and are parallel to substrate surface (so-called lateral interfaces). The physical processes underlying the lateral interface effects on functionalities of either the single-phase thin films or the superlattices, have been thoroughly investigated. For example, Grutter et al. observed interfacial ferromagnetism in superlattice of the paramagnetic metal $LaNiO_3$ and the antiferromagnetic insulator $CaMnO_3$.[3] It was believed that the ferromagnetism was attributed to a double exchange interaction among Mn ions mediated by the adjacent itinerant metal at the interface.

Compared to the long history of lateral interfaces, the interfaces in the vertically aligned nanocomposite films, which are perpendicular to substrate surface and so-called vertical interfaces, are rather a new and novel concept emerged in the past decade or so.[4−7] Such structure has powerful advantages over conventional lateral interfaces, such as easy interface probing, electrically addressable structure without patterning, and interfacial area much greater than substrate area etc.[8] However, significant obstacles to a systematic understanding of vertical interfaces still remain. Recently, we investigated the vertical interface effects in $(BiFeO_3)_{0.5}$:$(Sm_2O_3)_{0.5}$ composite films.[9,10] The strain generated at vertical interfaces has been revealed to be dominant factor determining lattice constants of $BiFeO_3$ and Sm_2O_3 phases. Hsieh et al. analyzed local leakage current located at the vertical interfaces of $BiFeO_3$:$CoFe_2O_4$ materials.[11] Their results clearly indicated that the enhanced conduction was observed at the interface region between $CoFe_2O_4$ pillar and $BiFeO_3$ matrix. On the basis of this local leakage behavior, a natural while critical question has been raised on how the vertical interfaces contribute to the conduction behavior of the entire thin film. The answer of this question is helpful to understand the physical mechanism underlying the vertical interface effects.

Leakage current has been well-known to be a main issue that limits the application of oxide thin films in memory devices.[12] How to reduce the leakage current is a long-term issue. In the present work, we investigated vertical interface effects on leakage behavior in $(BaTiO_3)_{0.5}$:$(Sm_2O_3)_{0.5}$ nanocomposite thin films. Compared to the pure $BaTiO_3$ (BTO) film, a largely reduced leakage current and a different leakage mechanism have been found in the composite films, which can be attributed to the aggregated oxygen vacancies at the vertical interfaces between BTO and Sm_2O_3.

Received: January 7, 2014
Accepted: March 31, 2014
Published: April 1, 2014

1. EXPERIMENTAL SECTION

Pulsed laser deposition (PLD) was used to fabricate $(BTO)_{0.5}$:$(Sm_2O_3)_{0.5}$ (BTO:Sm_2O_3) thin films on (001) $SrTiO_3$ (STO) and (001) Nb-doped $SrTiO_3$ (Nb-STO) substrates. A single ceramic pellet with a molar ratio of 0.5BTO-0.5Sm_2O_3 has been used as the target and was focused by a pulsed excimer laser (Lambda Physik, 248 nm, 3 Hz, 2 J/cm^2). Deposition temperature was 720 °C and oxygen pressure was 25 Pa. After deposition, the films have been annealed in situ at temperature of 450 °C and oxygen pressure of 0.8 atm for 1 h. For comparison, pure BTO and Sm_2O_3 thin films were fabricated using the same processing parameters. The crystal structure was investigated by X-ray diffraction (XRD, Rigaku K/Max) and transmission electron microscopy (TEM, FEI Tecnai F20 analytical microscope). The thickness was revealed by cross-sectional TEM. The surface morphology of the thin films was measured by atomic force microscope (AFM) with tapping mode at Asylum Research MFP-3D-SA. For electrical measurements, thin films with a thickness of ~200 nm were used. Top Pt electrodes with area of 8×10^{-4} cm^2 were fabricated by sputtering. A vertical capacitor structure of Pt/BTO:Sm_2O_3/Nb-STO has been used for electrical measurements. Current-voltage characteristics were measured by a Keithley 6517 analyzer. Bias polarity was defined as positive or negative based on the positive or negative voltage applied to the Pt electrode. The dielectric properties were investigated using an Agilent 4294A Impedence Analyzer. The measurements were performed at selected temperatures in a Linkam Scientific Instruments HFS600E-PB4 system.

2. RESULTS AND DISCUSSION

Figure 1 shows a typical XRD θ–2θ scan of the BTO: Sm_2O_3 thin film. It is obvious that the BTO and Sm_2O_3 phases are well-defined and have comparable intensities. Both of them show only (00l) diffraction peaks and hence is preferentially oriented along the c-axis. The in-plane orientation of the BTO:Sm_2O_3 films with respect to the major axis of the STO substrate is revealed by phi-scans (not shown). The orientation relationship is determined to be $(002)_{STO}//(002)_{BTO}//(002)_{Sm2O3}$ and $[020]_{STO}//[020]_{BTO}//[022]_{Sm2O3}$, which is in accordance with the pure BTO and Sm_2O_3 thin films grown on the STO substrates.[13] It should be pointed out that, because of the lattice mismatch between BTO and Sm_2O_3 (the out-of-plane lattice constants of bulk BTO and Sm_2O_3 are 4.034 and 10.93 Å, respectively), a large vertical strain of ~2.3% has been found in the BTO phase in the composite films which is comparable to the reported results.[14]

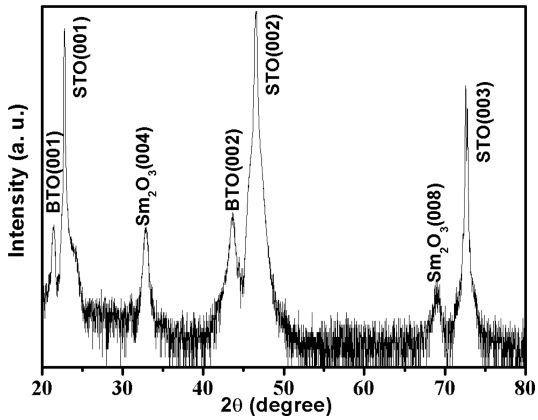

Figure 1. Typical XRD θ–2θ scan of the BTO:Sm_2O_3 thin film.

Figure 2 shows the surface morphology of (a) pure BTO, (b) BTO: Sm_2O_3, and (c) pure Sm_2O_3 thin films. The composite film clearly contains well-defined BTO (dark contrast) and Sm_2O_3 phases (light contrast). The different contrast originated from different elastic modulus (67 and 125 GPa for BTO and Sm_2O_3, respectively). The Sm_2O_3 phase has been found to distribute uniformly and exists as nanopillars or nanoparticles embedded in a BTO matrix, which is similar to that of BTO:$CoFe_2O_4$ composites.[15] The root-mean-square (rms) surface roughness of BTO, BTO:Sm_2O_3, and Sm_2O_3 films are determined to be 1.58, 2.69, and 2.70 nm, respectively.

To reveal the microstructure of BTO:Sm_2O_3 thin films, we performed cross-sectional TEM measurements and shown as Figure 3. As seen from the low-magnification bright-field TEM image (Figure 3a), the BTO and Sm_2O_3 are phase-separated, which is consistent with the XRD and AFM measurements. And their domains have self-assembled to be alternatively and vertically aligned, i.e., a spontaneous phase ordering of BTO and Sm_2O_3 with vertical nanostructure has formed. Combined with the AFM images, it is clear that Sm_2O_3 phase exists as nanopillars embedded in a BTO matrix. The composite nanostructure is believed to originate from a nucleation and growth process, which allows the surface energy of BTO matrix to be minimzed.[14] More than this, the interface strain and the surface step terrace are believed to contribute to the formation of vertical nanostructure.[16−21] Figure 3b shows the high-resolution TEM (HRTEM) image, which revealed excellent heteroepitaxial growth of BTO and Sm_2O_3 on the STO. The selected area diffraction (SAD, shown as Figure 3c) image revealed the same epitaxial relation as that from the XRD measurements. The epitaxy and spontaneous phase ordering between BTO and Sm_2O_3 in the composite thin film makes it a model system to explore the conceptual vertical interface effects in oxide thin films. The next key investigation is to explore the contribution of vertical interface to the conduction behavior of the entire thin film.

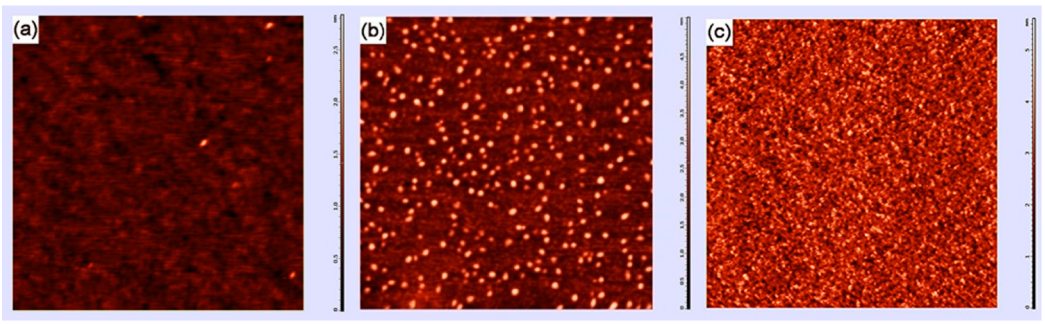

Figure 2. Surface morphology of (a) pure BTO, (b) BTO:Sm_2O_3, and (c) pure Sm_2O_3 thin films measured by AFM with tapping mode. The scan size is 2×2 μm^2.

dx.doi.org/10.1021/am5001129 | ACS Appl. Mater. Interfaces 2014, 6, 5356−5361

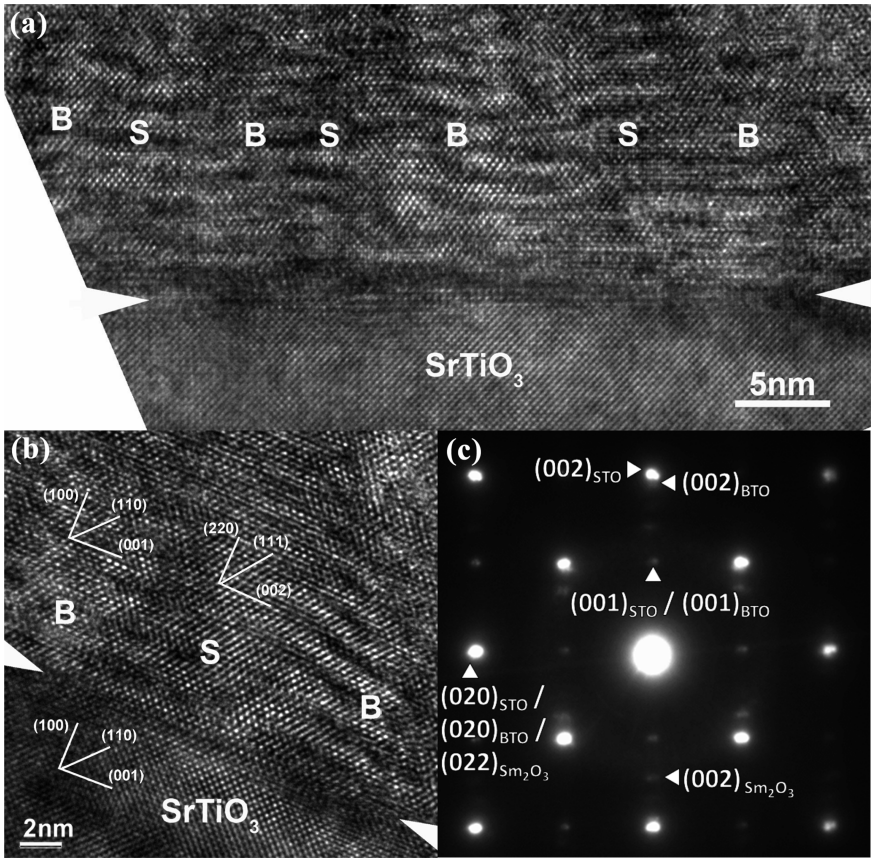

Figure 3. (a) Low-magnification TEM image, (b) high-resolution TEM image, and (c) selected area diffraction image of BTO:Sm_2O_3 thin films. B and S represent BTO and Sm_2O_3, respectively.

Hsieh et al. has reported the enhanced conduction at vertical interfaces in $BiFeO_3$:$CoFe_2O_4$ composite films.[11] A natural assumption is that the existence of the vertical interfaces may increase the leakage current of the entire thin film. While, the results shown as below indicate that the truth is exactly on the contrary. The inset a of Figure 4 shows the comparison of leakage current density of pure BTO and BTO:Sm_2O_3 thin films at room temperature. It is obviously that the leakage current density of composite thin films has been reduced by 2−3 orders of magnitude. This is a surprising result and it is important to understand the physics underlying the reduction.

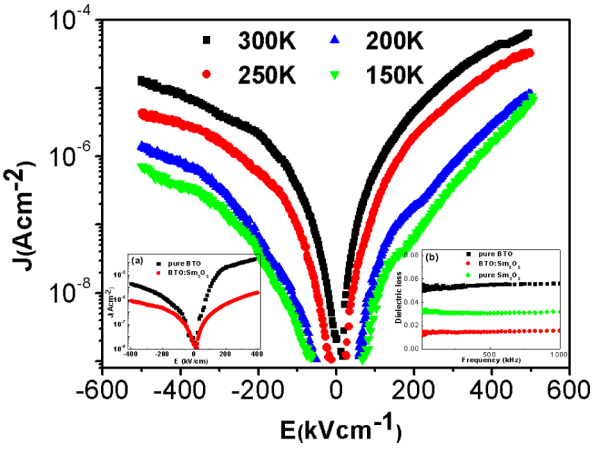

Figure 4. Temperature-dependent $J-E$ characteristics of BTO:Sm_2O_3 thin films from 150 to 300 K. Inset (a) shows the comparison of leakage current density of pure BTO and BTO:Sm_2O_3 thin films at room temperature. Inset (b) shows the dielectric loss of pure BTO, BTO:Sm_2O_3, and pure Sm_2O_3 films.

As indicated by the TEM images, there is a vertical nanostructure composed of alternative BTO and Sm_2O_3 columns in the composite films. And because a Pt/BTO:Sm_2O_3/Nb-STO vertical capacitor has been used in the electrical measurements, the total film can be reviewed as three resistors connected in parallel: the BTO phase, the Sm_2O_3 phase, and the vertical interfaces. Considering the high resistivity nature of the Sm_2O_3, the current is more like to go through the resistors of the BTO phase and the interfaces.[13] Furthermore, dielectric loss of pure BTO, BTO:Sm_2O_3, and pure Sm_2O_3 films have been measured and shown as inset (b) of Figure 4. A much lower value of BTO:Sm_2O_3 has been observed. On the basis of the strong relationship between the leakage current and the dielectric loss, the influence of the Sm_2O_3 phase on the leakage current of the entire BTO:Sm_2O_3 film can be neglected.[22]

To further investigate the function of the BTO phase and the vertical interfaces, the origin of leakage current, leakage mechanism, need to be analyzed. Different leakage mechanisms have been used to investigate the leakage current density-electric field ($J-E$) characteristics of dielectric oxide films: the space-charge-limited current (SCLC), the Poole−Frenkel (P−F) emission, the Schottky emission, and the Fowler-Nordheim (F−N) tunnelling.[23,24] The SCLC and P−F emission are bulk-limited conduction, where as the Schottky emission and F−N tunneling are interface-limited conduction. In the present work, the temperature dependent $J-E$ curves of pure BTO has been

dx.doi.org/10.1021/am5001129 | ACS Appl. Mater. Interfaces 2014, 6, 5356−5361

measured and the dominant leakage mechanisms have been revealed to be Schottky emission and F−N tunneling at positive and negative biases, respectively (not shown). These results are consistent with previous report.[25] Figure 4 shows temperature-dependent $J-E$ characteristics of BTO:Sm_2O_3 thin films from 150 to 300 K. For a fixed electric field, the J decreases with decreasing temperature, which is typical for dielectric oxide thin films. We point out that we considered all four mechanisms in the present work, but only the proper mechanism is discussed in more details below.

Figure 5 shows $\ln(J)$ vs $\ln(E)$ curves for the BTO:Sm_2O_3 thin film at a negative bias. The plots show a linear behavior

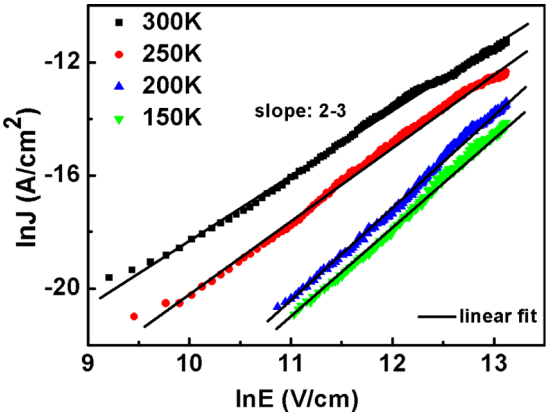

Figure 5. Ln(J) vs ln(E) curves for BTO:Sm_2O_3 thin films at a negative bias.

with a slope at the range of 2−3 in almost the whole measured electric field, in agreement with the trap-controlled SCLC mechanism. When the current was mainly affected by the space-chargers, the leakage mechanism is named as SCLC and can be described by Child's law[23,26]

$$J \propto \varepsilon_r \varepsilon_0 \mu \frac{E^\alpha}{L} \quad (1)$$

where ε_r is the relative dielectric constant, ε_0 is the permittivity of free space, μ is the charge carrier mobility, L is the film thickness, and α is a trap-dependent exponential factor. For the SCLC with no traps, α equals to 2. While for trap-controlled SCLC, α drivatives from 2.[27] It is well-known that μ is determined mainly by impurity scattering at low-temperature range and can be described as $\mu \propto T^{3/2}$, which contributed to the decreased J with decreasing temperature.[28] It should be pointed out that a $\ln(J)$ vs $\ln(E)$ analysis at positive bias at these temperatures yields the similar results (not shown).

As we discussed earlier, the SCLC is a typical bulk-limited conduction. In other words, the conduction behavior in the BTO:Sm_2O_3 thin films is only correlated with the film itself other than the top and bottom electrodes. These are obviously different from the interface-limited conduction behavior, Schottky emission and F−N tunneling, in the pure BTO films. The different leakage mechanism indicates that the vertical interfaces other than the BTO phase is the one who dominate the leakage behavior in composite films. Now we turn to understanding the reduced leakage current in the BTO:Sm_2O_3 thin films.

Oxygen vacancies (V_Os) are intrinsic defects in oxide thin films and play an essential role in determining leakage current in dielectric materials, such as BTO and $BiFeO_3$.[22,25,29,30] V_Os have been approved to accumulate at the interfaces because of the structural discontinuity as well as the strain.[31−37] Considering the large lattice mismatch and a high strain generated at the interfaces in the present work, the vertical interfaces are believed to become the sinks to attract the V_Os.[11,38] The accumulation of V_Os reduced the leakage current of BTO phase in the composite film compared to that of the pure BTO, which contribute to the reduction of leakage current and dielectric loss of the entire BTO:Sm_2O_3 film. More than this, the accumulated V_Os can be reviewed as ions with positive space charges.[39,40] As we discussed earlier, the leakage current went through the vertical interfaces other than the BTO and Sm_2O_3 phases in the composite film. During the conduction process, the V_Os acted as potential wells and trapped the carriers (electrons) through the interfaces. On the other hand, the carrier mobility at the vertical interfaces is lowered due to the high density of disorders. Therefore, a largely reduced leakage current and a trap-controlled SCLC mechanism are the result.[41]

3. CONCLUSIONS

In conclusion, a spontaneous phase ordering with clear vertical interfaces has been found in the BTO:Sm_2O_3 composite thin films which were used as a model system to understand the vertical interface effects of oxide thin films. A largely reduced leakage current as well as a different leakage mechanism has been found in the composite films compared to that of the pure BTO film. The structural discontinuity and a high strain contributed to the accumulation of V_Os at the interfaces, which originated to the different conduction behavior in the BTO:Sm_2O_3 thin films. Our work represented a technique to reduce the leakage current in BTO thin films and hold great promise for other dielectric oxide materials. More interestingly, it suggested that the vertical interfaces can be reviewed as not only the medium to generating strain but also a conduction pathway in the nanocomposite films.

AUTHOR INFORMATION

Corresponding Author

*E-mail: yanghao@suda.edu.cn.

Notes

The authors declare no competing financial interest.

ACKNOWLEDGMENTS

The authors acknowledge the support of the National Natural Science Foundation of China (Grants 11004145, 11274237, 51228201, and 51202153), the Natural Science Foundation of Jiangsu Province under Grant BK2010223, the Scientific Research Foundation for the Returned Overseas Chinese Scholars (State Education Ministry of China), and the Priority Academic Program Development of Jiangsu Higher Education Institutions (PAPD). The TEM work at Texas A&M University is funded by the U.S. National Science Foundation (NSF-1007969).

REFERENCES

(1) Hwang, H. Y.; Iwasa, Y.; Kawasaki, M.; Keimer, B.; Nagaosa, N.; Tokura, Y. Emergent Phenomena at Oxide Interfaces. *Nat. Mater.* **2012**, *11*, 103−113.

(2) Zubko, P.; Gariglio, S.; Gabay, M.; Ghosez, P.; Triscone, J. M. Interface Physics in Complex Oxide Heterostructures. *Annu. Rev. Condens. Matter Phys.* **2011**, *2*, 141−165.

(3) Grutter, A. J.; Yang, H.; Kirby, B. J.; Fitzsimmons, M. R.; Aguiar, J. A.; Browning, N. D.; Jenkins, C. A.; Arenholz, E.; Mehta, V. V.; Alaan, U. S.; Suzuki, Y. Interfacial Ferromagnetism in $LaNiO_3$/$CaMnO_3$ Superlattices. *Phys. Rev. Lett.* **2013**, *111*, 087202.
(4) Moshnyaga, V.; Damaschke, B.; Shapoval, O.; Belenchuk, A.; Faupel, J.; Lebedev, O. I.; Verbeeck, J.; Tendeloo, G.; Van Mucksch, M.; Tsurkan, V.; Tidecks, R.; Samwer, K. Structural Phase Transition at the Percolation Threshold in Epitaxial $(La_{0.7}Ca_{0.3}MnO_3)_{1-x}$:$(MgO)_x$ Nanocomposite Films. *Nat. Mater.* **2003**, *2*, 247−252.
(5) Zheng, H.; Wang, J.; Lofland, S. E.; Ma, Z.; Mohaddes-Ardabili, L.; Zhao, T.; Salamanca-Riba, L.; Shinde, S. R.; Ogale, S. B.; Bai, F.; Viehland, D.; Jia, Y.; Schlom, D. G.; Wuttig, M.; Roytburd, A.; Ramesh, R. Multiferroic $BaTiO_3$-$CoFe_2O_4$ Nanostructures. *Science* **2004**, *303*, 661−663.
(6) Chen, A. P.; Bi, Z. X.; Tsai, C. F.; Lee, J. H.; Su, Q.; Zhang, X. H.; Jia, Q. X.; MacManus-Driscoll, J. L.; Wang, H. Tunable Low-Field Magnetoresistance in $(La_{0.7}Sr_{0.3}MnO_3)_{0.5}$:$(ZnO)_{0.5}$ Self-Assembled Vertically Aligned Nanocomposite Thin Films. *Adv. Funct. Mater.* **2011**, *21*, 2423−2429.
(7) Chen, A. P.; Bi, Z. X.; Jia, Q. X.; MacManus-Driscoll, J. L.; Wang, H. Microstructure, Vertical Strain Control and Tunable Functionalities in Self-Assembled, Vertically Aligned Nanocomposite Thin Films. *Acta Mater.* **2013**, *61*, 2783−2792.
(8) MacManus-Driscoll, J. L. Self-Assembled Heteroepitaxial Oxide Nanocomposite Thin Film Structures: Designing Interface-Induced Functionality in Electronic Materials. *Adv. Funct. Mater.* **2010**, *20*, 2035−2045.
(9) MacManus-Driscoll, J. L.; Zerrer, P.; Wang, H.; Yang, H.; Yoon, J.; Fouchet, A.; Yu, R.; Blamire, M. G.; Jia, Q. X. Strain Control and Spontaneous Phase Ordering in Vertical Nanocomposite Heteroepitaxial Thin Films. *Nat. Mater.* **2008**, *7*, 314−320.
(10) Yang, H.; Wang, H.; Yoon, J.; Wang, Y. Q.; Jain, M.; Feldmann, D. M.; Dowden, P. C.; MacManus-Driscoll, J. L.; Jia, Q. X. Vertical Interface Effect on the Physical Properties of Self-Assembled Nanocomposite Epitaxial Films. *Adv. Mater.* **2009**, *21*, 3794−3798.
(11) Hsieh, Y. H.; Liou, J. M.; Hwang, B. H.; Liang, C. W.; He, Q.; Zhan, Q.; Chiu, Y. P.; Chen, Y. C.; Chu, Y. H. Local Conduction at the $BiFeO_3$-$CoFe_2O_4$ Tubular Oxide Interface. *Adv. Mater.* **2012**, *24*, 4564−4568.
(12) Chambers, S. A. Epitaxial Growth and Properties of Doped Transition Metal and Complex Oxide Films. *Adv. Mater.* **2010**, *22*, 219−248.
(13) Yang, H.; Wang, H.; Luo, H. M.; Feldmann, D. M.; Dowden, P. C.; Depaula, R. F.; Jia, Q. X. Structural and Dielectric Properties of Epitaxial Sm_2O_3 Thin Films. *Appl. Phys. Lett.* **2008**, *92*, 062905.
(14) Harrington, S. A.; Zhai, J.; Denev, S.; Gopalan, V.; Wang, H.; Bi, Z. X.; Redfern, S. A. T.; Baek, S. H.; Bark, C. W.; Eom, C. B.; Jia, Q. X.; Vickers, M. E.; MacManus-Driscoll, J. L. Thick Lead-Free Ferroelectric Films with High Curie Temperatures through Nanocomposite-Induced Strain. *Nat. Nanotechnol.* **2011**, *6*, 491−494.
(15) Zheng, H.; Straub, F.; Yang, P. L.; Hsieh, W. K.; Zavaliche, F.; Chu, Y. H.; Dahmen, U.; Ramesh, R. Self-Assembled Growth of $BiFeO_3$−$CoFe_2O_4$ Nanostructures. *Adv. Mater.* **2006**, *18*, 2747−2752.
(16) Jiang, J. C.; Henry, L. L.; Gnanasekar, K. I.; Chen, C. L.; Meletis, E. I. Self-Assembly of Highly Epitaxial (La, Sr)MnO_3 Nanorods on (001) $LaAlO_3$. *Nano Lett.* **2004**, *4*, 741−745.
(17) Jiang, J. C.; Meletis, E. I.; Asuvathraman, R.; Govindan Kutty, K. V.; Gnanasekar, K. I.; Chen, C. L. Self-Assembled Three-Dimensional Epitaxial Ionic Fluorite $Gd_2Zr_2O_7$ Nanorods on (001) $LaAlO_3$. *Appl. Phys. Lett.* **2005**, *86*, 163110.
(18) Jiang, J. C.; Meletis, E. I.; Yuan, Z.; Chen, C. L. Interface Modulated Structure of Highly Epitaxial (Pb, Sr)TiO_3 Thin Films on (001) MgO. *Appl. Phys. Lett.* **2007**, *90*, 051904.
(19) Liu, M.; Ma, C. R.; Collins, G.; Liu, J.; Chen, C. L.; Dai, C.; Lin, Y.; Shui, L.; Xiang, F.; Wang, H.; He, J.; Jiang, J. C.; Meletis, E. I.; Cole, M. W. Interface Engineered $BaTiO_3$/$SrTiO_3$ Heterostructures with Optimized High-Frequency Dielectric Properties. *ACS Appl. Mater. Interfaces* **2012**, *4*, 5761−5765.
(20) Ma, C. R.; Liu, M.; Chen, C. L.; Lin, Y.; Li, Y. R.; Horwitz, J. S.; Jiang, J. C.; Meletis, E. I.; Zhang, Q. Y. The Origin of Local Strain in Highly Epitaxial Oxide Thin Films. *Sci. Rep.* **2013**, *3*, 3092.
(21) He, J.; Jiang, J. C.; Meletis, E. I.; Liu, M.; Liu, J.; Collins, G.; Ma, C. R.; Chen, C. L.; Bhalla, A. Evolution of Nano-fingers in Epitaxial Mn-Doped Ba(Zr,Ti)O_3 Thin Films Driven by {110} Twin Boundaries. *Philos. Mag. Lett.* **2011**, *91*, 361.
(22) Wang, C.; Takahashi, M.; Fujino, H.; Zhao, X.; Kume, E.; Horiuchi, T.; Sakai, S. Leakage Current of Multiferroic $(Bi_{0.6}Tb_{0.3}La_{0.1})FeO_3$ Thin Films Grown at Various Oxygen Pressures by Pulsed Laser Deposition and Annealing Effect. *J. Appl. Phys.* **2006**, *99*, 054104.
(23) Dietz, G. W.; Antpohler, W.; Klee, M.; Waser, R. Electrode Influence on the Charge Transport through $SrTiO_3$ Thin Films. *J. Appl. Phys.* **1995**, *78*, 6113.
(24) Ahn, K. H.; Kim, S. S.; Baik, S. G. Change of Conduction Mechanism by Microstructural Variation in Pt/(Ba, Sr)TiO_3/Pt Film Capacitors. *J. Appl. Phys.* **2002**, *92*, 421.
(25) Yang, H.; Tao, K.; Chen, B.; Qiu, X. G.; Xu, B.; Zhao, B. R. Leakage Mechanism of $(Ba_{0.7}Sr_{0.3})TiO_3$ Thin Films in the Low-Temperature Range. *Appl. Phys. Lett.* **2002**, *81*, 4817.
(26) Boer, K. W. *Survey of Semiconductor Physics*; Van Nostrand Reinhold: New York, 1990.
(27) Shang, D. S.; Wang, Q.; Chen, L. D.; Dong, R.; Li, X. M.; Zhang, W. Q. Effect of Carrier Trapping on the Hysteretic Current-Voltage Characteristics in Ag/$La_{0.7}Ca_{0.3}MnO_3$/Pt Heterostructures. *Phys. Rev. B* **2006**, *73*, 245427.
(28) Sze, S. M. *Physics of Semiconductor Devices*, 2nd ed; Wiley: New York, 1981.
(29) Li, W. W.; Zhao, R.; Wang, L.; Tang, R. T.; Zhu, Y. Y.; Lee, J. H.; Cao, H. X.; Cai, T. Y.; Guo, H. Z.; Wang, C.; Ling, L. S.; Pi, L.; Jin, K. J.; Zhang, Y. H.; Wang, H.; Wang, Y.; Ju, S.; Yang, H. Oxygen-Vacancy-Induced Antiferromagnetism to Ferromagnetism Transformation in $Eu_{0.5}Ba_{0.5}TiO_{3-\delta}$ Multiferroic Thin Films. *Sci. Rep.* **2013**, *3*, 2618.
(30) Qi, X.; Dho, J.; Tomov, R.; Blamire, M. G.; MacManus-Driscoll, J. L. Greatly Reduced Leakage Current and Conduction Mechanism in Aliovalent- Ion-Doped $BiFeO_3$. *Appl. Phys. Lett.* **2005**, *86*, 062903.
(31) Klenov, D. O.; Donner, W.; Foran, B.; Stemmer, S. Impact of Stress on Oxygen Vacancy Ordering in Epitaxial $(La_{0.5}Sr_{0.5})$-$CoO_{3-\delta}$Thin Films. *Appl. Phys. Lett.* **2003**, *82*, 3427.
(32) Cuong, D. D.; Lee, B.; Choi, K. M.; Ahn, H. S.; Han, S. W.; Lee, J. C. Oxygen Vacancy Clustering and Electron Localization in Oxygen-Deficient $SrTiO_3$: LDA+U Study. *Phys. Rev. Lett.* **2007**, *98*, 115503.
(33) Wimbush, S. C.; Li, M.; Vickers, M. E.; Maiorov, B.; Feldmann, D. M.; Jia, Q. X.; MacManus-Driscoll, J. L. Interfacial Strain-Induced Oxygen Disorder as the Cause of Enhanced Critical Current Density in Superconducting Thin Films. *Adv. Funct. Mater.* **2009**, *19*, 835−841.
(34) Torija, M. A.; Sharma, M.; Gazquez, J.; Varela, M.; He, C.; Schmitt, J.; Borchers, J. A.; Laver, M.; El-Khatib, S.; Leighton, C. Chemically Driven Nanoscopic Magnetic Phase Separation at the $SrTiO_3(001)$/$La_{1-x}Sr_xCoO_3$ Interface. *Adv. Mater.* **2011**, *23*, 2711−2715.
(35) Donner, W.; Chen, C.; Liu, M.; Jacobson, A. J.; Lee, Y. L.; Gadre, M.; Morgan, D. Epitaxial Strain-Induced Chemical Ordering in $La_{0.5}Sr_{0.5}CoO_{3-\delta}$ Films on $SrTiO_3$. *Chem. Mater.* **2011**, *23*, 984−988.
(36) Gazquez, J.; S. Bose, S.; M. Sharma, M.; M. A. Torija, M. A.; S. J. Pennycook, S. J.; C. Leighton, C.; M. Varela, M. Lattice Mismatch Accommodation via Oxygen Vacancy Ordering in Epitaxial $La_{0.5}Sr_{0.5}CoO_{3-\delta}$ Thin Films. *APL Mater.* **2013**, *1*, 012105.
(37) Pennycook, S. J.; Zhou, H.; Chisholm, M. F.; Boriserich, A. Y.; Varela, M.; Gazauez, J.; Pennycook, T. J.; Narayan, J. Misfit Accommodation in Oxide Thin Film Heterostructures. *Acta Mater.* **2013**, *61*, 2725−2733.
(38) Fix, T.; Choi, E. M.; Robinson, J. W. A.; Lee, S. B.; Chen, A. P.; Prasad, B.; Wang, H.; Blamire, M. G.; MacManus-Driscoll, J. L. Electric-Field Control of Ferromagnetism in a Nanocomposite via a ZnO Phase. *Nano Lett.* **2013**, *13*, 5886−5890.

(39) Muller, D. A.; Nakagawa, N.; Ohtomo, A.; Grazul, J. L.; Hwang, H. Y. Atomic-Scale Imaging of Nanoengineered Oxygen Vacancy Profiles in $SrTiO_3$. *Nature* **2004**, *430*, 657−661.
(40) Mizokawa, T.; Wakisaka, Y.; Sudayama, T.; Iwai, C.; Miyoshi, K.; Takeuchi, J.; Wadati, H.; Hawthern, D. G.; Regier, T. Z.; Sawatzky, G. A. Role of Oxygen Holes in Li_xCoO_2 Revealed by Soft X-Ray Spectroscopy. *Phys. Rev. Lett.* **2013**, *111*, 056404.
(41) Tredgold, R. H. *Space Charge Conduction in Solids*; Elsevier: Amsterdam, 1966.